

1 Article

2 Anti-fibrotic effect of Smad decoy 3 oligodeoxynucleotide in CCl₄-induced hepatic 4 fibrosis animal model

5 Mi-Gyeong Gwon ¹, Jung-Yeon Kim ¹, Hyun-Jin An ¹, Woon-Hae Kim ¹, Hyemin Gu ¹,
6 Min-Kyung Kim ², Sok Cheon Pak ³ and Kwan-Kyu Park ^{1,*}

7 ¹ Department of Pathology, College of Medicine, Catholic University of Daegu, 33, Duryugongwon-ro 17-gil,
8 Nam-gu, Daegu 42472, Korea; daldy88@cu.ac.kr (M.-G.G.); jy1118@cu.ac.kr (J.-Y.K.); ahj119@cu.ac.kr (H.-J.A.);
9 kimwoonhae@cu.ac.kr (W.-H.K.); guhm1207@cu.ac.kr (H.G.)

10 ² Department of pathology, Dongguk University School of Medicine, Gyeongju 38066, Republic of Korea;
11 minkyungk76@naver.com (M.-K.K.)

12 ³ School of Biomedical Sciences, Charles Sturt University, Panorama Avenue, Bathurst, NSW 2795, Australia;
13 spak@csu.edu.au (S.-C.P.)

14 * Correspondence: kkpark@cu.ac.kr; Tel.: +82-53-650-4149

15
16
17
18 **Abstract:** Hepatic fibrosis is the wound-healing process of chronic hepatic disease that leads to
19 end-stage of hepatocellular carcinoma and demolition of hepatic structures. EMT has been identified
20 to phenotypic conversion of the epithelium to mesenchymal phenotype that occurred during
21 fibrosis. Smad decoy oligodeoxynucleotide (ODN) is a synthetic DNA fragment containing
22 complementary sequence of Smad transcription factor. Thus, this study evaluated the anti-fibrotic
23 effects of Smad decoy ODN on carbon tetrachloride (CCl₄)-induced hepatic fibrosis in mice. As
24 shown in histological results, CCl₄ treatment triggered hepatic fibrosis and increased Smad
25 expression. On the contrary, Smad decoy ODN administration suppressed fibrogenesis and EMT
26 process. The expression of Smad signaling and EMT-associated protein was markedly decreased in
27 Smad decoy ODN treatment mice compared with CCl₄-injured mice. In conclusion, these data
28 indicate the practicability of Smad decoy ODN administration for preventing hepatic fibrosis and
29 EMT processes.

30 Key word: liver fibrosis; Smad; decoy; oligodeoxynucleotide; CCl₄

31

32

33

34 **1. Introduction**

35 The liver is the main organ of immense complexity responsible for the metabolism of drugs and
36 toxic chemicals [1]. Chronic liver diseases affecting hundreds of millions of people globally are
37 associated with a developed progress of hepatocellular carcinoma and hepatic fibrosis [2]. Hepatic
38 fibrosis is a consequence of wound-healing responses of the liver that is caused by chronic liver
39 injuries such as alcoholic, viral and autoimmune hepatitis [3]. Regardless of causes, direct and
40 sustained hepatic injury induces a persistent inflammatory response and excessive deposition of
41 extracellular matrix (ECM) in the perisinusoidal space of Disse, leading to the progression of hepatic
42 fibrosis [4]. Hepatic fibrogenesis affects both hepatocytes and non-parenchymal cells such as hepatic
43 stellate cells (HSCs), which are prerequisite for preserving an entire liver structure and function [5].

44 Hepatocyte and HSCs as the major source of myofibroblasts in injured liver play an important
45 role in the progress of liver inflammation and development of hepatic fibrosis. Any chronic form of
46 hepatic injury can result in transformation of hepatocytes into mesenchymal cells by an
47 epithelial-mesenchymal transition (EMT) process. EMT is dynamic process in which fully
48 differentiated epithelial cells undergo a phenotypic change, resulting in loss of marker proteins such
49 as E-cadherin and zonula occludens-1(ZO-1), and acquisition of mesenchymal characteristics such as
50 α -SMA, vimentin, matrix metalloproteinase (MMP)-2, MMP-9 and collagens [6, 7]. In addition,
51 following damage to the epithelial cells, bile duct epithelium and hepatocytes released the
52 profibrogenic cytokine that further activates HSCs [8, 9]. The activated HSCs lead to hepatic
53 fibrogenesis by excessively production of ECM components such as type I collagen and fibronectin
54 [8,9].

55 Carbon tetrachloride (CCl₄), a classic hepatotoxic agent, is commonly used to induce liver injury
56 in experimental animal model to examine the pathogenesis of fibrosis and hepatic cirrhosis [1]. This
57 liver injury is ascribed to inflammation originating from CCl₄-derived trichloromethylperoxy free
58 radical formation in the liver [10]. CCl₄ treatment induces centrilobular necrosis which causes a
59 wound-healing response that starts with recruitment of inflammatory and phagocytic cells
60 recruitment in liver necrotic zones, then accumulation of ECM, release of fibrotic cytokines. Finally,
61 continued hepatic inflammatory responses provoked by prolonged CCl₄ administration is believed
62 to induce hepatic fibrosis, cirrhosis, and hepatocellular carcinoma [11-13].

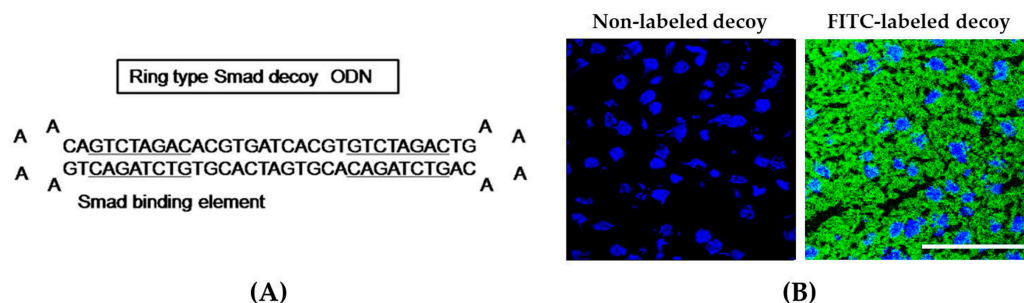
63 Many studies have identified that a variety of cytokines and growth factors, including
64 transforming growth factor- β 1 (TGF- β 1), epidermal growth factor (EGF) and hepatocyte growth
65 factor (HGF), participate in EMT process [6, 14, 15]. TGF- β 1/Smad signaling has been reported as a
66 mechanism leading to hepatic fibrosis. TGF- β 1 activates Smad-dependent and Smad-independent
67 pathways to display its biological activities. For Smad-dependent pathways, TGF- β 1 exerts diverse
68 biological activities via its intracellular mediators Smad2 and Smad3, and is negatively regulated by
69 an inhibitory mediator Smad7 [16]. Smads have been also identified to interact with other pathways
70 such as the MAPK and NF- κ B signaling pathways [17]. However, these cellular signaling processes
71 still remain unclear in the hepatocytes. Therefore, a recent review concentrates on the regulatory
72 mechanisms and functional role of TGF- β 1/Smad pathway during the progression of hepatic fibrosis
73 [18].

74 Decoy oligodeoxynucleotide (ODN) is a synthetic short DNA segment containing a consensus
75 binding sequence that competitively combines with target transcription factor [19]. As a result, the
76 decoy ODN binds to the specific transcription factor and inhibits gene expression by preventing the
77 upregulation of involved genes. We previously demonstrated that inhibition of Smad and Sp1 by the
78 decoy ODN strategy prevented renal fibrosis in mice via inhibition of the production of cytokines
79 related to fibrosis and EMT [20]. Additionally, we examined that anti-fibrotic effect NF- κ B decoy
80 ODN in hepatic fibrosis [21]. However, the effect of Smad ODN on hepatic fibrosis in hepatocyte has
81 not been reported. Therefore, we investigated the anti-fibrotic effect of Smad decoy ODN on hepatic
82 fibrosis by regulating a Smad signaling pathway and EMT process, using CCl₄-induced hepatic
83 fibrosis.

85 **2. Results**86 **2.1. Transfection efficiency and DNA-binding activity of Smad decoy ODN in the CCl₄-treated mouse liver**

87 We designed ring type Smad decoy ODN and synthesized double stranded ODN that contains
88 the sequence Smad binding element (Fig 1A). To identify the successful transfer of Smad decoy
89 ODN, we analyzed the transfection efficiency of the FITC-labeled ODN using fluorescence
90 microscopy. FITC-labeled Smad ODNs were administered intravenously and detected by
91 fluorescence were shown in cytoplasm and nucleus of liver cells (Fig. 1B). These results indicate that
92 Smad decoy ODN was successfully transfected into mouse liver.

93



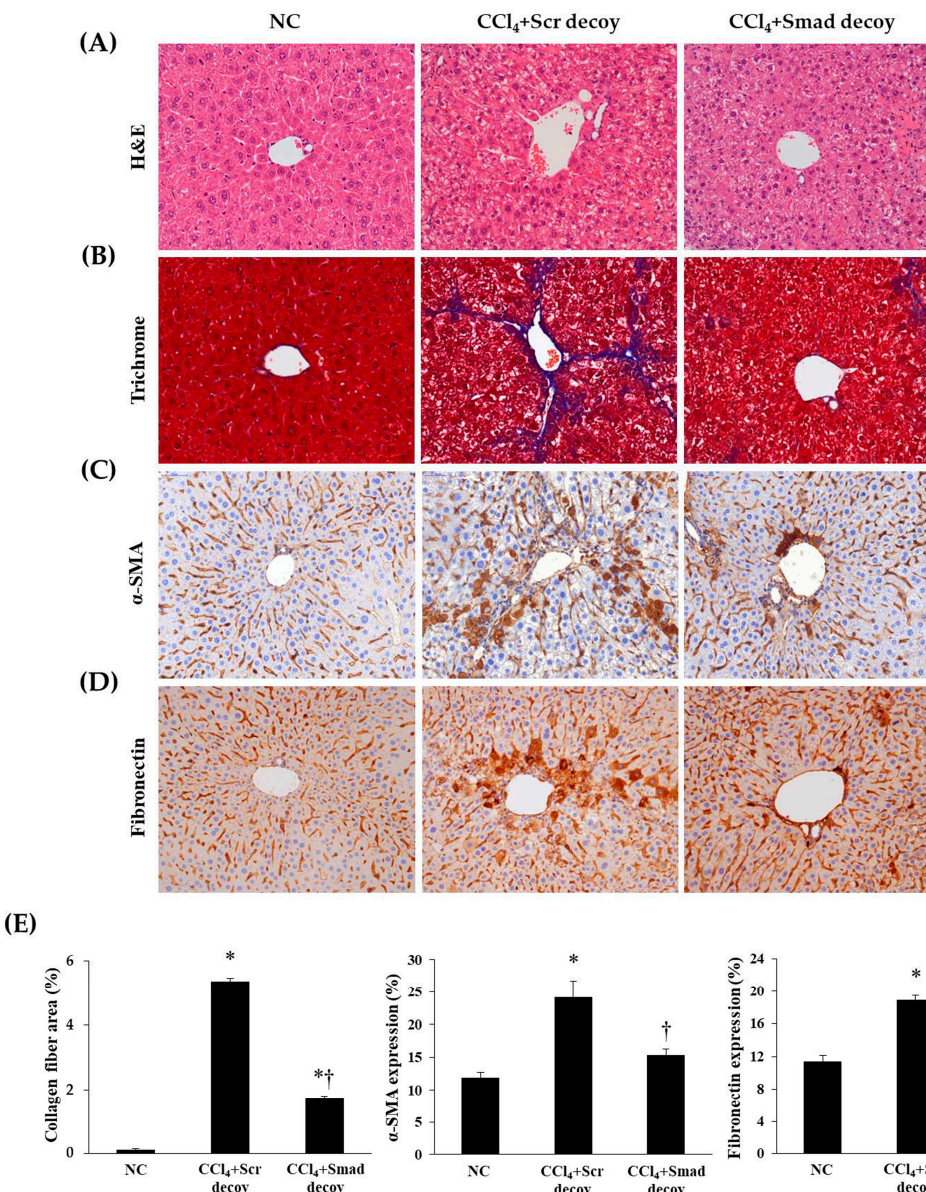
94

95 **Fig 1. Synthesis of Smad decoy oligodeoxynucleotide (ODN) and transfection of Smad decoy**
96 **ODN into mouse liver.** (A) Design of ring-type Smad decoy ODN including GTCTAGAC which is
97 the consensus sequence for the Smad binding element; (B) Immunofluorescence image of the
98 transfer effect of Smad decoy ODN in liver of mice. The image on the left is the result of
99 administration of non-labeled ODN and the image on the right green fluorescence represented
100 successful transfection into mouse liver. Scale bar, 50 μ m.

101

102 **2.2. Smad decoy ODN attenuated morphological changes in CCl₄-induced hepatic fibrosis**

103 CCl₄ administration induced centrilobular necrosis, proliferation of parenchymal cells and
104 non-parenchymal cells, fibrosis and accumulation of ECM [18]. To identify anti-fibrotic effect of
105 Smad decoy ODN in hepatic fibrogenesis, we used CCl₄-induced hepatotoxic model. To show
106 histological change, we performed both H&E staining (Fig 2A) and Masson's trichrome staining (Fig
107 2B). The basic lobular architecture was well preserved with portal vein in the normal control group.
108 Cellular inflammation, ballooning changes of hepatocytes and lobular necrosis had developed
109 around the sinusoids in CCl₄-treated mouse. These changes were significantly attenuated by Smad
110 decoy ODN treatment. Additionally, Smad decoy ODN was able to prevent the accumulation of
111 collagen caused by CCl₄-induced liver damage. Taken together, these data indicate that Smad decoy
112 ODN suppressed morphological changes and collagen accumulation in the CCl₄-injected mice.



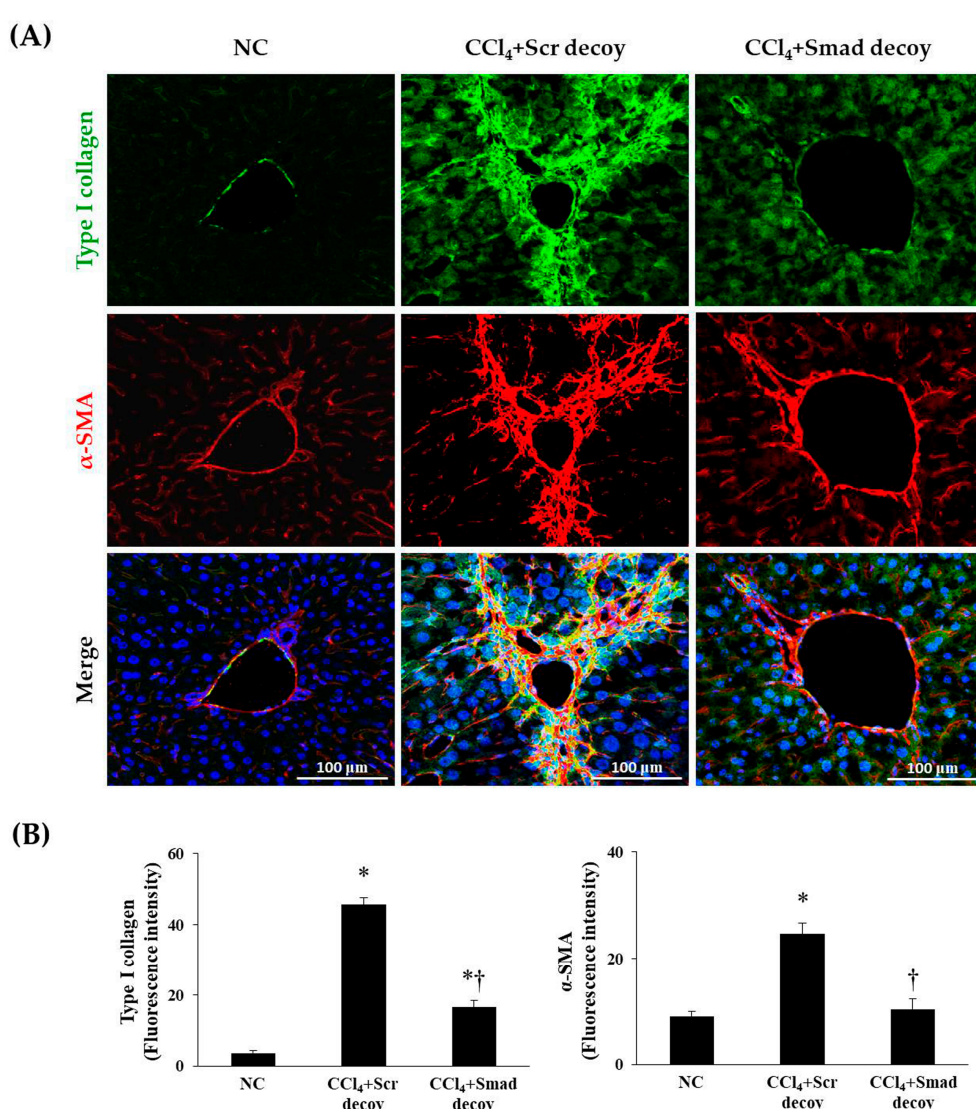
113
114 **Fig 2. Smad decoy ODN attenuated morphological changes in CCl₄-induced hepatic fibrosis in**
115 **mice.** Paraffin-embedded liver section stained with H&E staining (A), Masson's trichrome staining
116 (B); As a mesenchymal marker, α -SMA (C) and fibronectin (D) was detected by
117 immunohistochemical staining; (E) Quantification of collagen, α -SMA and fibronectin expressions
118 CCl₄ increased expression of α -SMA whereas Smad decoy ODN downregulated it. Original
119 magnification, $\times 400$. * $p < 0.05$ compared to normal control group; † $p < 0.05$ compared to the
120 CCl₄+Scr group.

121

122 2.3. Smad decoy ODN suppressed ECM accumulation and EMT process in CCl₄-induced hepatic fibrosis

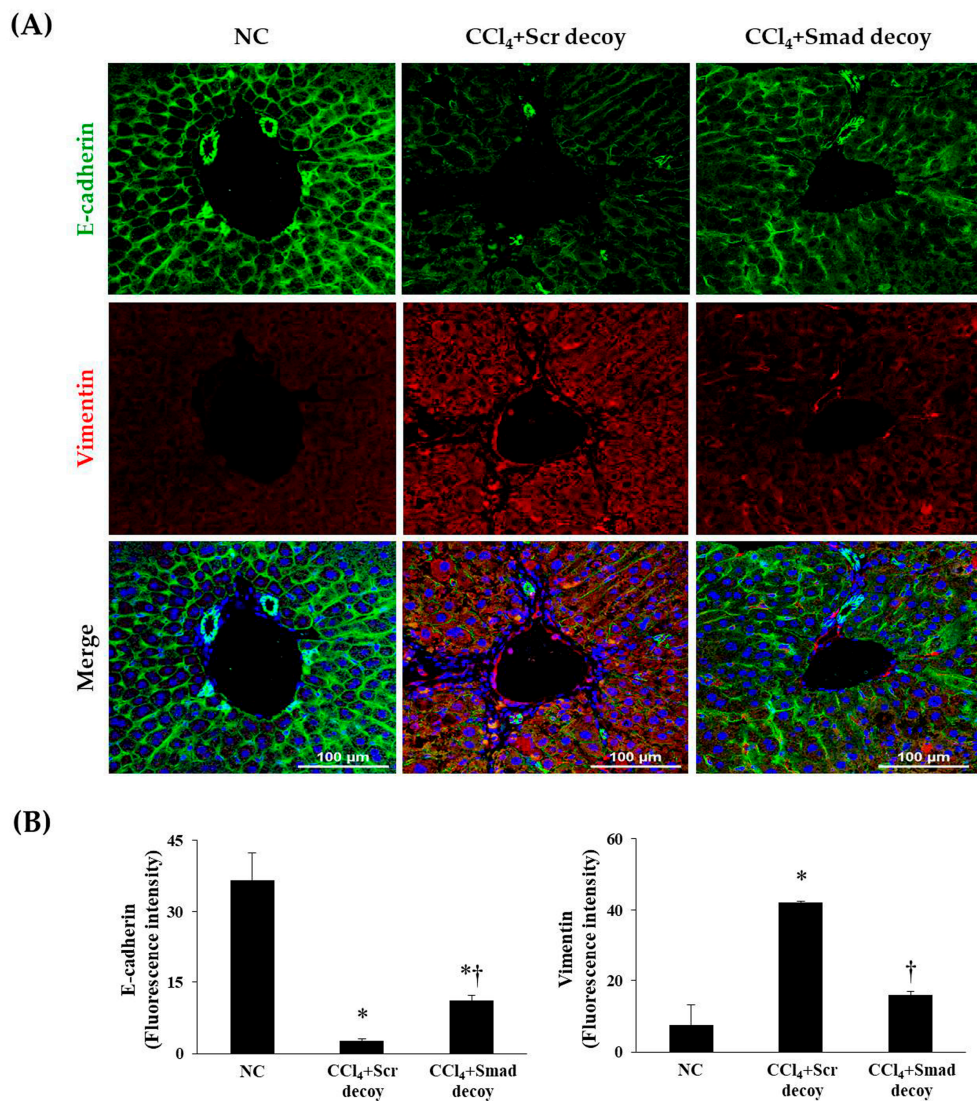
123 Following liver injury, hepatic stellate cell undergo phenotypic changes which leads to
124 increased deposition of ECM proteins, such as α -SMA, fibronectin and type I collagen in the hepatic
125 sinusoid [21]. Therefore, we investigated the effects of Smad decoy ODN on hepatic fibrogenesis and
126 ECM accumulation by immunohistochemical and immunofluorescent staining in CCl₄-induced
127 hepatic fibrosis. The expression of α -SMA as a mesenchymal marker was obviously elevated in
128 CCl₄-injured mice compared with normal mice. However, the administration of Smad decoy ODN
129 resulted in downregulation of α -SMA expression (Fig 2C). The expression of fibronectin within the
130 liver sinusoid increased in CCl₄-induced fibrosis mice, whereas administration of Smad decoy
131 suppressed fibronectin expression (Fig 2D). The effect of Smad decoy ODN on CCl₄-induced fibrosis

132 in the liver was further investigated by immunofluorescent staining. The expression of α -SMA and
 133 type I collagen was increased in the liver tissue of the CCl_4 -injured mice, but this increase was
 134 inhibited by Smad decoy ODN (Fig 3).
 135



136
 137 **Fig 3. Expression of extracellular matrix (ECM) decreased by Smad decoy ODN in CCl_4 -induced**
 138 **hepatic fibrosis in mice.** Immunofluorescence double staining for type I collagen (green) and
 139 α -SMA (red) showed that Smad decoy ODN administration suppressed ECM deposition around of
 140 portal vein. The nuclei were stained with Hoechst. Magnification, $\times 400$.

141
 142 During the EMT in hepatic fibrosis, intercellular junctions of epithelial cells are disrupted by
 143 down-regulation of E-cadherin which is confirmed by increase of mesenchymal phenotype,
 144 including vimentin [22]. As shown in Figure 4, the expression of E-cadherin in immunofluorescence
 145 was decreased after CCl_4 injury compared with normal control, and vimentin showed the opposite
 146 result. However, Smad decoy ODN administration suppressed this expression change in the fibrotic
 147 liver. These findings show that Smad decoy ODN has anti-fibrotic properties through
 148 downregulation of ECM expression and disruption of EMT process following liver injury.



149

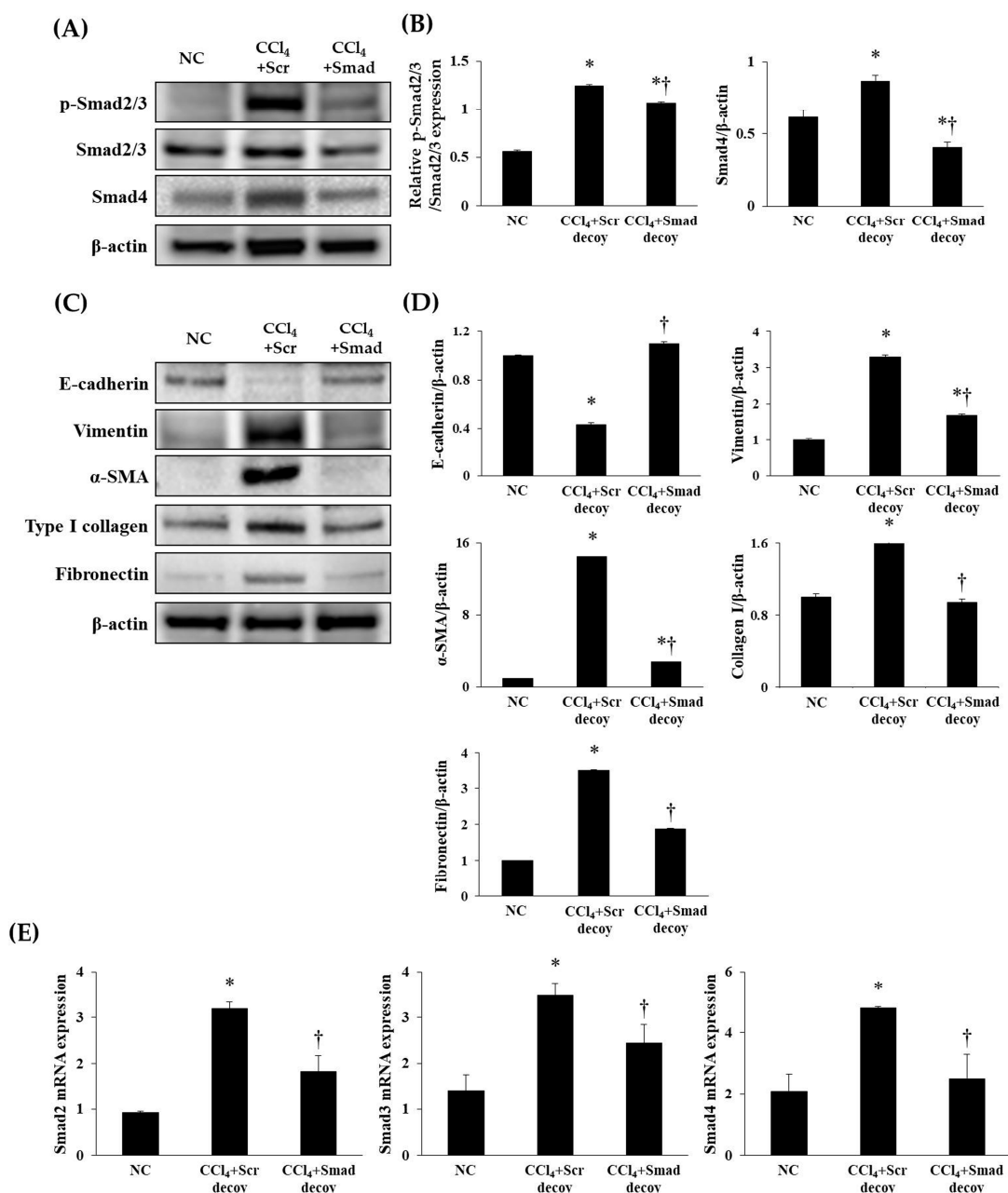
150 **Fig 4. Effect of Smad decoy ODN on the expression of Epithelial to mesenchymal transition**
151 **(EMT).** Representative immunofluorescence staining showed that Smad ODN administration
152 increased expression of E-cadherin (green) and decreased expression of vimentin (red) around of
153 portal vein of hepatic fibrosis in mice. To counterstain, the nuclei were labeled with Hoechst
154 33342(blue). Image magnification, $\times 400$.

155

156 2.4. *Smad decoy ODN inhibited fibrotic genes by regulating Smad-dependent signaling pathway in*
157 *CCl₄-induced hepatic fibrosis*

158 TGF- β 1/Smad signaling has been found to be a crucial mediator in EMT and subsequent
159 fibrosis. A rapid relocation of Smad proteins by TGF- β 1 signaling is followed by transcription of
160 fibrogenesis gene [23]. To investigate the regulation of Smad decoy ODN on TGF- β 1 downstream
161 signaling pathway, we investigated the expression of p-Smad2/3 and Smad4 by Western blotting.
162 The expressions of p-Smad2/3 and Smad4 were markedly increased in hepatic fibrosis mice
163 compared with normal mice ($p < 0.05$, Fig 5A and B). However, injection of Smad decoy ODN
164 attenuated CCl₄-induced fibrotic mediator production through suppression of binding Smad
165 transcription factor in DNA binding site. In addition, quantitative real-time PCR (qRT-PCR) data
166 shown that Smad decoy ODN inhibit Smad signaling pathway (Fig 5E). Next, fibrogenesis and EMT
167 expression levels in the fibrotic liver were measured by Western blot (Fig 5C and D). Western blot
168 results showed that the expression of vimentin, α -SMA, fibronectin, and type I collagen increased in
169 fibrotic liver compared to normal control mice ($p < 0.05$). However, Smad ODN administration

170 decreased the tissue vimentin, α -SMA, type I collagen and fibronectin levels. On the other hand, The
 171 CCl_4 inhibited E-cadherin expression while a relative amount of E-cadherin was preserved in Smad
 172 decoy ODN treated livers. These results indicate that Smad decoy ODN inhibits hepatic EMT and
 173 fibrosis via blocking TGF- β 1-stimulted Smad signaling pathway in CCl_4 -induced hepatic fibrosis.



174
 175 **Fig 5. Synthetic Smad decoy ODN significantly suppressed fibrotic genes and ECM proteins by**
 176 **blocking Smad-dependent signaling pathway.** (A) Western blot analysis showed that Smad decoy
 177 ODN suppressed the expression of p-Smad2/3 and Smad4. All samples were loaded the equal
 178 volumes, which was confirmed by loading GAPDH together; The results are representative of three
 179 independent experiments; (B) The expression levels of the protein from quantification of these
 180 images by Image J. The expressions of E-cadherin, vimentin, α -SMA, type I collagen and fibronectin
 181 as the representative of three independent experiments (C) and quantification of ECM proteins (D);
 182 (E) qRT-PCR analysis showed that Smad decoy ODN inhibited the mRNA expression of Smad2,
 183 Smad3 and Smad4. * $p < 0.05$ compared to normal control group; † $p < 0.05$ compared to the CCl_4 +Scr
 184 group.
 185

186 **3. Discussion**

187 Hepatic fibrosis is a complicated pathological process of several chronic liver diseases. Many
188 studies have underlined the potentiality of the Smad signaling group participation in the
189 pathogenesis of hepatic fibrosis and carcinogenesis (fibro-carcinogenesis) [24, 25]. Smad proteins a
190 central role in the transduction of receptor signals to target genes in the nucleus [26].

191 Decoy ODN is a double-stranded DNA segment containing a specific transcription factor
192 binding element [19]. Some studies reported that the induction of synthetic decoy ODN with high
193 attraction for their target transcription factors into peculiar cells. A previous study demonstrated
194 that NF- κ B decoy ODN inhibited the EMT process in mice of CCl₄-induced hepatic fibrosis [21]. Park
195 et al. [27] reported the effect of ring-type decoy ODNs on CCl₄-induced hepatic fibrosis. Their study
196 showed that a ring-type Sp1 decoy ODN suppressed the level of cytokines, TGF- β 1 downstream
197 target genes and hepatic fibrosis. However, anti-fibrotic effect of Smad decoy ODN in hepatic
198 fibrosis has not yet been demonstrated. Thus, in the current study, we synthesized Smad decoy
199 ODN and investigated the effect of Smad decoy ODN on hepatic fibrosis. The Smad decoy ODN
200 used in this study was a synthesized double-stranded ODN containing the consensus Smad binding
201 element (GTCTAGAC) that binds with Smad 2/3/4 complex. In our previous study, we
202 demonstrated that synthetic decoy ODN was effectively transfected into hepatocytes [21]. On the
203 basis of the results of our previous study, we investigated the effect of Smad decoy ODN on
204 CCl₄-induced hepatic fibrosis. With this aim in mind, Smad decoy ODN was transfected into liver
205 cells.

206 The CCl₄-induced hepatic fibrosis model is commonly used for anti-fibrotic research with many
207 studies showing that CCl₄, hepatotoxic agent, activated the TGF- β 1/Smad signaling pathway and led
208 to accumulation of ECM [21, 28]. Increased TGF- β 1 initiated intracellular signaling by binding
209 TGF- β receptor type II and TGF- β 1 then stimulated TGF- β receptor type I kinase, resulting in
210 activation of the downstream signaling pathway [29, 30]. Following binding of TGF- β 1 to receptors,
211 Smad2 and Smad3 were phosphorylated by TGF- β receptors and its complex with Smad4. This
212 transcription factor complex was translocated to the nucleus. Complexes of p-Smad2/3 and Smad4 in
213 the nucleus can regulate the transcription of the fibrous gene [31]. Thus, to identify anti-fibrotic
214 effect of Smad decoy ODN, we used CCl₄ hepatotoxic animal model. Consistent with previous
215 study, our research show that CCl₄ hepatotoxic agent accumulated ECM components and activated
216 TGF- β 1 signaling. In addition, the expression levels of p-Smad2/3 and Smad4 was increased by CCl₄,
217 and Smad decoy ODN decreased them. In the present study, the hepatotoxic agent CCl₄ stimulated
218 increased expression of ECM proteins and activated Smad-dependent signaling. However, Smad
219 decoy ODN decreased the expression of type I collagen, α -SMA and fibronectin.

220 The Smad-dependent signaling response was correlated with the EMT process during hepatic
221 fibrogenesis. In addition, Sung et al. [20] demonstrated that inhibition of Smad signaling attenuated
222 the EMT process and accumulation of ECM in renal fibrosis. Some research also suggested that
223 chronic hepatic injury resulted in transformation of hepatocytes into myofibroblasts by the EMT
224 process [32]. During EMT, symptoms such as increased migratory capacity, invasiveness, enhanced
225 resistance to apoptosis and greatly increased ECM production occur. EMT has been classified into
226 three dissimilar biological subtypes built on biological circumstances. The type 2 EMT, classified as
227 organ fibrosis, is associated with organ repair and is involved in secondary morphologic change of
228 epithelial or endothelial cells to resident mesenchymal or fibroblast cells in response to persistent
229 inflammation. This processes lead to loss of epithelial marker proteins and acquisition of
230 mesenchymal characteristics [7]. In present study, the epithelial markers decreased and
231 myofibroblast markers increased by CCl₄ administration. It suggested that hepatocytes changed into
232 myofibroblasts via the EMT process. However, this result can be interpreted differently. For
233 example, loss of E-cadherin may have been the result of CCl₄-induced hepatocyte injury, and
234 proliferation of myofibroblasts may have occurred in response to hepatocyte-secreted cytokines. In
235 addition, several studies investigated that there is a contradiction in the EMT process [33]. The
236 controversy surrounding the EMT process means that it has become one of the most debated topics

237 in hepatic fibrosis study today [34]. In current study, we just investigated the anti-fibrotic effect of
238 Smad decoy ODN and observed the EMT processes in an animal model of hepatic fibrosis.
239 Therefore, to support inhibition effect of Smad decoy ODN on EMT process more experiment needs
240 through *in vivo* and *in vitro*.

241 In summary, this study confirmed that Smad decoy ODN inhibited hepatic fibrosis by blocking
242 the TGF- β 1/Smad signaling pathway which was activated by CCl₄ administration. CCl₄-treated mice
243 induced inflammation response and hepatic failure such as accumulation of ECM, centrilobular
244 necrosis, activation of fibrotic genes and EMT processes. However, effectively transfection of Smad
245 decoy ODN attenuated immune responses and pathophysiological changes in the liver. But, in our
246 study, only the histological examination was carried out, and thus it is considered that further study
247 on the expression level of cytokine is needed. In addition, Smad decoy ODN suppressed EMT
248 processes and the production of ECM proteins in CCl₄-induced hepatic fibrosis. Therefore, these
249 results indicate that Smad decoy ODN is able to protect liver against hepatic injury.

250 Taken together, our results demonstrate that Smad decoy ODN suppressed Smad-mediated
251 hepatic fibrosis by blocking Smad signaling pathway and reducing EMT processes. Given this fact,
252 Smad decoy ODN gene therapy might provide a new therapeutic strategy to prevent hepatic
253 fibrosis. However, more studies are needed to further determine the relationship between the
254 therapeutic use of Smad signaling and hepatic fibrosis to chronic hepatic diseases.

255 4. Materials and Methods

256 4.1. Synthesis of ring-type Smad decoy ODNs

257 Decoy ODNs were synthesized by Macrogen (Seoul, Korea). Smad and scrambled (Scr) decoy
258 ODN sequences used were listed below in Table 1 (consensus sequence is underlined). This section
259 is not mandatory, but can be added to the manuscript if the discussion is unusually long or complex.

260 **Table 1.** Sequences of decoy used in this study

Decoy	Sequence
Scr	5'-GAATTCAATT CAGGGTACGGCA AAAAATTGCCGTACCC TGA ATT-3'
Smad	5'- GAATT CGT TCTAGACTGAAA ACAGT CTAGACAC-3'

261 These structures were annealed for 6 h, while temperature was decreased from 80 °C to 25°C. These
262 decoy ODNs were predicted to form a stem-loop structure (Figure 1). To obtain a covalent ligation
263 for ring-type decoy ODN molecules, each decoy ODN was mixed with T4 ligase (Takara Bio, Otsu,
264 Japan) and incubated for 18 h at 16°C.

266 4.2. Animal models and Smad decoy ODN transfer

268 Animal protocols were approved by the Institutional Animal Care and Use Committee of the
269 Catholic University of Daegu (EXP-IRB number: 2014-0001-CU-AEC-04-A). Male C57BL/6 mice (6
270 weeks old, 20-22g; Samtako, Daejeon, South Korea) were housed in a room with controlled humidity
271 and temperature, and a 12h light-dark cycle. To examine the *in vivo* transfection efficiency of
272 synthetic Scr ODN, Smad decoy ODN and FITC-labeled Smad decoy ODN were injected into mice
273 intravenously (using the tail vein). The mice were sacrificed 24 h after injection. Optimum cutting
274 temperature compound (Sakura Finetek Japan, Tokyo, Japan) was used to embed liver tissue
275 samples prior to frozen sectioning. Cryosections of liver, which were transferred with FITC-labeled
276 Smad decoy ODN, were examined by fluorescence microscopy.

277 Mice were randomly divided into three groups as follows: (1) normal control (NC) group, (2)
278 group treated with CCl₄ and Scr decoy ODN (CCl₄+Scr), and (3) group treated with CCl₄ and Smad
279 decoy ODN (CCl₄+Smad). Chronic liver injuries were induced by intraperitoneal injection of CCl₄ (2
280 ml/kg, dissolved in corn oil [at a ratio of 1:3] three times a week.

281 One week after the first CCl₄ injection, Scr or Smad decoy ODN (10 μ g) was transferred
282 biweekly via the mouse tail vein, using an in vivo gene delivery system (Mirus Bio, Madison, WI,
283 USA). Mice were sacrificed 8 weeks after the first CCl₄ injection. All experiments were anesthetized
284 with Isoflurane (O₂ 0.5 L/min, Isoflurane 2%) inhalation anesthesia and Avertin (2, 2,
285 2-Tribromoethanol + 2-methyl-2-butanol + Saline Mix → After Filter 250 mg/kg intraperitoneal
286 administration) to reduce animal pain. When the animal suffers an unbearable pain, it was
287 euthanized using CO₂.

288
289 *4.3. Histology analysis*

290 All liver tissues were fixed in 10% formalin at room temperature. After fixation, sections
291 perpendicular to the anterior-posterior axis of the liver were dehydrated in graded ethanol, cleared
292 in xylene, and embedded in paraffin. Paraffin-embedded tissues were cut into 4 μ m sections and
293 deparaffinized. Liver tissue sections were stained with hematoxylin and eosin (H&E) and Masson's
294 trichrome according to standard protocol.

295
296 *4.4. Immunohistochemical staining*

297 Paraffin-embedded sections were deparaffinized with xylene and dehydrated in gradually
298 decreasing concentrations of ethanol. For immunohistochemical analysis, the dehydrated tissue
299 sections were immersed in a 10mM sodium citrate buffer (pH 6.0) for 5 min at 95°C. The last step was
300 repeated using a fresh 10 mM sodium citrate solution (pH 6.0). The sections were allowed to remain
301 in the same solution while cooling for 20 min, and they were then rinsed in phosphate-buffered
302 saline (PBS). Next, sections were incubated with a primary antibody (1:100 dilution) for 1h at 37 °C.
303 Primary antibodies were follows: anti-fibronectin (BD Biosciences, Burlington, Canada) and
304 anti- α -SMA (A2547, Sigma-Aldrich, St.Louis, MO, USA). After three serial washes with PBS, the
305 sections were processed by an indirect immunoperoxidase technique using a commercial Envision
306 System kit (DAKO, Carpinteria, CA, USA). Immunohistochemical images were viewed with an
307 Eclipse 80i microscope (Nikon, Tokyo, Japan).

308
309 *4.5. Immunofluorescent staining*

310 Paraffin-embedded liver tissue sections were deparaffinized with xylene and dehydrated in
311 gradually decreasing concentrations of ethanol. Tissue sections were then placed in blocking serum
312 (10% donkey serum) at room temperature for 1 h. The sections were immunostained with primary
313 antibodies (1:500 dilution) against type I collagen (Novous Biologicals, Littleton, CO, USA),
314 E-cadherin (Cell Signaling Technology, Danvers, MA, USA), Vimentin (BD Biosciences) and α -SMA
315 (Abcam) at room temperature for 2h. After washing, sections were incubated with the secondary
316 antibodies (1:200 dilution) conjugated with Alexa Fluor 488 or Alexa Fluor 555 (Thermo Fisher
317 Scientific, Waltham, MA, USA) for 30 min at 37 °C. Slides were then mounted using Dako
318 fluorescence mounting medium. Specimens were examined and photographed with a confocal
319 microscope (Nikon, Tokyo, Japan).

320
321 *4.6. Western blot analysis*

322 Frozen liver tissues were homogenized in cell lyticTM M lysis reagent (Sigma-Aldrich, St.Louis,
323 MO, USA) and samples were centrifuged at 12,000 rpm for 20 min at 4°C after incubation for 30 min
324 on ice. The supernatant was collected, and the residual protein concentration was determined by
325 using Bradford assay (Bio-Rad Laboratories, Hercules, CA, USA). Total protein was separated on 8%
326 to 12% sodium dodecyl sulfate polyacrylamide gels and transferred to nitrocellulose membrane (GE
327 Healthcare, Little Chalfont, Buckinghamshire, UK) using the standard SDS-PAGE procedure. The
328 membranes were blocked in 5% bovine serum albumin in TBS-T (10 mM Tris, 150 mM NaCl, and

329 0.1% Tween-20) for 1 h at room temperature. Then, the membrane was probed with a primary
 330 antibody (1:1000 dilution) overnight at 4 °C. The membrane was further probed with horseradish
 331 peroxidase conjugated secondary antibody (1:2000 dilution) for 2 h at room temperature. The signals
 332 were detected using an enhanced chemiluminescence detection system (Amersham, Piscataway, NJ,
 333 USA). The primary antibodies used were anti-fibronectin, anti-vimentin (BD Biosciences),
 334 anti-p-Smad2/3, anti-Smad2/3, anti-Smad4 (Santa Cruz Biotechnology, Santa Cruz, CA, USA),
 335 anti-type I collagen (Novous Biologicals), anti- α -SMA (Abcam), anti-E-cadherin (Cell Signaling
 336 Technology), and anti-glyceraldehyde-3-phosphate-dehydrogenase (GAPDH) (Cell Signaling
 337 Technology).

338

339 *4.7. Qiamtotatove real-time PCR (qRT-PCR)*

340 Total RNA was isolated from liver tissues using TRIzol Reagent (Thermo Fisher Scientific,
 341 Waltham, MA, USA) according to the manufacturer's recommendations. Reverse transcription
 342 reaction was performed by using AccuPower RT Premix and Oligo dT18 primer (Bioneer, Daejeon,
 343 Korea) according to the manufacturer's recommendations. The PCR mixtures contained 100ng of
 344 cDNA and 100pM each of forward and reverse primers. The samples were denatured at 95C for 10
 345 min, followed by 45 cycles of annealing and extension at 95 °C for 20s, 60 °C for 20s, and 72 °C for 20s.
 346 Real-time PCR was performed in a LightCycler nano System (Roche Applied Science, Mannheim,
 347 Germany) by using LightCycler DNA Master SYBR GREEN I (Roche Applied Science). Expression
 348 values were normalized to β -actin. The real-time PCR was performed in a LightCycler nano System
 349 (Roche Applied Science, Mannheim, Germany) by using LightCycler DNA Master SYBR GREEN I
 350 (Roche Applied Science). The primer sequences were as follows:

351

Table 2. Sequences of PCR primer used in this study

Gene	Sequence
Smad2	forward, 5'-TGCATTCTGGTGTCAATCG -3' reverse 5'-CGAGTTGATGGGTCTGTGA -3'
Smad3	forward 5'-GTCAACAAAGTGGTGGCGTG-3' reverse 5'-GCAGCAAAGGCTTCTGGGATAA-3'
Smad4	forward 5'-TGACGCCCTAACCAATTCCAG-3' reverse 5'-CTCCTAAGAGCAAGGCAGCAAA-3'

352

353 *4.8. Statistical analysis*

354 All data are presented as means \pm SE. A Student's t-test was used to assess the significance of
 355 independent experiments. Differences with $p < 0.05$ were considered significant.

356

357 **Author Contributions:** Mi-Gyeong Gwon, Jung-Yeon Kim and Kwan-Kyu Park conceived and designed the
 358 experiments; Mi-Gyeong Gwon and Jung-Yeon Kim is co-first author. Mi-Gyeong Gwon, Jung-Yeon Kim,
 359 Hyun-Jin An, Woon-Hae Kim, Hyemin Gu performed the experiments; Min-Kyung Kim, Sok-choen Park
 360 discussed the study and analyzed the data. All authors have read and approved the final version of this
 361 manuscript.

362 **Acknowledgments:** This work was supported by the National Research Foundation of Korea grant funded by
 363 the Korean Government (NRF-2015R1D1A1A01061026).

364 **Conflicts of Interest:** The authors declare no conflict of interest.

365

366 References

367

368 1. Tan, H.; He, Q.; Li, R.; Lei, F.; Lei, X. Trillin Reduces Liver Chronic Inflammation
369 and Fibrosis in Carbon Tetrachloride (CCl₄) Induced Liver Injury in Mice.
370 *Immunological investigations* **2016**, *45*, 371-82.

371 2. Friedman, S. L. Evolving challenges in hepatic fibrosis. *Nature reviews. Gastroenterology & hepatology* **2010**, *7*, 425-36.

372 3. Friedman, S. L. Molecular regulation of hepatic fibrosis, an integrated cellular
373 response to tissue injury. *The Journal of biological chemistry* **2000**, *275*, 2247-50.

374 4. Bataller, R.; Brenner, D. A. Liver fibrosis. *The Journal of clinical investigation* **2005**, *115*, 209-18.

375 5. Weiler-Normann, C.; Herkel, J.; Lohse, A. W. Mouse models of liver fibrosis.
376 *Zeitschrift fur Gastroenterologie* **2007**, *45*, 43-50.

377 6. Wu, T.; Chen, J. M.; Xiao, T. G.; Shu, X. B.; Xu, H. C.; Yang, L. L.; Xing, L. J.;
378 Zheng, P. Y.; Ji, G. Qinggan Huoxue Recipe suppresses epithelial-to-mesenchymal
379 transition in alcoholic liver fibrosis through TGF-beta1/Smad signaling pathway. *World
380 journal of gastroenterology* **2016**, *22*, 4695-706.

381 7. Lee, W. R.; Kim, K. H.; An, H. J.; Kim, J. Y.; Lee, S. J.; Han, S. M.; Pak, S. C.; Park,
382 K. K. Apamin inhibits hepatic fibrosis through suppression of transforming growth
383 factor beta1-induced hepatocyte epithelial-mesenchymal transition. *Biochemical and
384 biophysical research communications* **2014**, *450*, 195-201.

385 8. Seki, E.; de Minicis, S.; Inokuchi, S.; Taura, K.; Miyai, K.; van Rooijen, N.;
386 Schwabe, R. F.; Brenner, D. A. CCR2 promotes hepatic fibrosis in mice. *Hepatology*
387 **2009**, *50*, 185-97.

388 9. Friedman, S. L. Hepatic Fibrosis: Emerging Therapies. *Dig Dis* **2015**, *33*, 504-7.

389 10. Son, G.; Iimuro, Y.; Seki, E.; Hirano, T.; Kaneda, Y.; Fujimoto, J. Selective
390 inactivation of NF-kappaB in the liver using NF-kappaB decoy suppresses CCl₄-induced
391 liver injury and fibrosis. *American journal of physiology. Gastrointestinal and liver
392 physiology* **2007**, *293*, G631-9.

393 11. Britton, R. S.; Bacon, B. R. Role of free radicals in liver diseases and hepatic
394 fibrosis. *Hepato-gastroenterology* **1994**, *41*, 343-8.

395 12. Parola, M.; Robino, G. Oxidative stress-related molecules and liver fibrosis. *Journal
396 of hepatology* **2001**, *35*, 297-306.

397 13. Wu, J.; Norton, P. A. Animal models of liver fibrosis. *Scandinavian journal of
398 gastroenterology* **1996**, *31*, 1137-43.

399 14. Wendt, M. K.; Schiemann, W. P. Therapeutic targeting of the focal adhesion
400 complex prevents oncogenic TGF-beta signaling and metastasis. *Breast cancer research
401 : BCR* **2009**, *11*, R68.

402 15. Tian, M.; Neil, J. R.; Schiemann, W. P. Transforming growth factor-beta and the
403 hallmarks of cancer. *Cellular signalling* **2011**, *23*, 951-62.

404 16. Lan, H. Y.; Chung, A. C. Transforming growth factor-beta and Smads.
405 *Contributions to nephrology* **2011**, *170*, 75-82.

406 17. Deryck, R.; Zhang, Y. E. Smad-dependent and Smad-independent pathways in
407 TGF-beta family signalling. *Nature* **2003**, *425*, 577-84.

408 18. Xu, F.; Liu, C.; Zhou, D.; Zhang, L. TGF-beta/SMAD Pathway and Its Regulation
409 in Hepatic Fibrosis. *The journal of histochemistry and cytochemistry : official journal of
410 the Histochemistry Society* **2016**, *64*, 157-67.

411 19. Morishita, R.; Sugimoto, T.; Aoki, M.; Kida, I.; Tomita, N.; Moriguchi, A.; Maeda,
412 K.; Sawa, Y.; Kaneda, Y.; Higaki, J.; Ogihara, T. In vivo transfection of cis element
413 "decoy" against nuclear factor-kappaB binding site prevents myocardial infarction.
414 *Nature medicine* **1997**, *3*, 894-9.

415

416

417 20. Sung, W. J.; Kim, K. H.; Kim, Y. J.; Chang, Y. C.; Lee, I. H.; Park, K. K.
418 Antifibrotic effect of synthetic Smad/Sp1 chimeric decoy oligodeoxynucleotide through
419 the regulation of epithelial mesenchymal transition in unilateral ureteral obstruction
420 model of mice. *Experimental and molecular pathology* **2013**, *95*, 136-43.

421 21. Kim, K. H.; Lee, W. R.; Kang, Y. N.; Chang, Y. C.; Park, K. K. Inhibitory effect of
422 nuclear factor-kappaB decoy oligodeoxynucleotide on liver fibrosis through regulation
423 of the epithelial-mesenchymal transition. *Human gene therapy* **2014**, *25*, 721-9.

424 22. Grunert, S.; Jechlinger, M.; Beug, H. Diverse cellular and molecular mechanisms
425 contribute to epithelial plasticity and metastasis. *Nature reviews. Molecular cell biology*
426 **2003**, *4*, 657-65.

427 23. Shrestha, N.; Chand, L.; Han, M. K.; Lee, S. O.; Kim, C. Y.; Jeong, Y. J. Glutamine
428 inhibits CCl₄ induced liver fibrosis in mice and TGF-beta1 mediated
429 epithelial-mesenchymal transition in mouse hepatocytes. *Food and chemical toxicology : an international journal published for the British Industrial Biological Research Association* **2016**, *93*, 129-37.

430 24. Friedman, S. L. Liver fibrosis -- from bench to bedside. *Journal of hepatology* **2003**,
431 *38 Suppl 1*, S38-53.

432 25. Matsuzaki, K. Smad phosphoisoform signals in acute and chronic liver injury:
433 similarities and differences between epithelial and mesenchymal cells. *Cell and tissue
434 research* **2012**, *347*, 225-43.

435 26. Bran, G. M.; Sommer, U. J.; Goessler, U. R.; Hormann, K.; Riedel, F.; Sadick, H.
436 TGF-ss1 antisense impacts the SMAD signalling system in fibroblasts from keloid scars.
437 *Anticancer research* **2010**, *30*, 3459-63.

438 27. Park, J. H.; Jo, J. H.; Kim, K. H.; Kim, S. J.; Lee, W. R.; Park, K. K.; Park, J. B.
439 Antifibrotic effect through the regulation of transcription factor using ring type-Sp1
440 decoy oligodeoxynucleotide in carbon tetrachloride-induced liver fibrosis. *The journal of
441 gene medicine* **2009**, *11*, 824-33.

442 28. Zeisberg, M.; Yang, C.; Martino, M.; Duncan, M. B.; Rieder, F.; Tanjore, H.;
443 Kalluri, R. Fibroblasts derive from hepatocytes in liver fibrosis via epithelial to
444 mesenchymal transition. *The Journal of biological chemistry* **2007**, *282*, 23337-47.

445 29. Conidi, A.; Cazzola, S.; Beets, K.; Coddens, K.; Collart, C.; Cornelis, F.; Cox, L.;
446 Joke, D.; Dobreva, M. P.; Dries, R.; Esguerra, C.; Francis, A.; Ibrahimi, A.; Kroes, R.;
447 Lesage, F.; Maas, E.; Moya, I.; Pereira, P. N.; Stappers, E.; Stryjewska, A.; van den
448 Berghe, V.; Vermeire, L.; Verstappen, G.; Seuntjens, E.; Umans, L.; Zwijsen, A.;
449 Huylebroeck, D. Few Smad proteins and many Smad-interacting proteins yield multiple
450 functions and action modes in TGFbeta/BMP signaling in vivo. *Cytokine & growth
451 factor reviews* **2011**, *22*, 287-300.

452 30. Xie, F.; Zhang, Z.; van Dam, H.; Zhang, L.; Zhou, F. Regulation of TGF-beta
453 Superfamily Signaling by SMAD Mono-Ubiquitination. *Cells* **2014**, *3*, 981-93.

454 31. Zhao, Y. L.; Zhu, R. T.; Sun, Y. L. Epithelial-mesenchymal transition in liver
455 fibrosis. *Biomedical reports* **2016**, *4*, 269-274.

456 32. Copple, B. L. Hypoxia stimulates hepatocyte epithelial to mesenchymal transition
457 by hypoxia-inducible factor and transforming growth factor-beta-dependent
458 mechanisms. *Liver international : official journal of the International Association for the
459 Study of the Liver* **2010**, *30*, 669-82.

460 33. Taura, K.; Miura, K.; Iwaisako, K.; Osterreicher, C. H.; Kodama, Y.;
461 Penz-Osterreicher, M.; Brenner, D. A. Hepatocytes do not undergo
462 epithelial-mesenchymal transition in liver fibrosis in mice. *Hepatology* **2010**, *51*,
463 1027-36.

464

465

466 34. Taura, K.; Iwaisako, K.; Hatano, E.; Uemoto, S. Controversies over the
467 Epithelial-to-Mesenchymal Transition in Liver Fibrosis. *Journal of clinical medicine*
468 **2016**, *5*.